RSC Advances

ROYAL SOCIETY OF CHEMISTRY

www.rsc.org/advances

Target-Responsive dumbbell probe-mediated rolling circle amplification strategy for highly sensitive Hg^{2+} detection

Qingwang Xue [a], Yanqin Lv [a], Yuanfu Zhang [a], Shuling Xu [a], Qiaoli Yue [a], Rui Li [a], Lei Wang [a], Haibo Li [a], Xiaohong Gu [b], Shuqiu Zhang[b], Jifeng Liu [a]*

[a] *Department of Chemistry, Liaocheng University, Liaocheng, 252059, Shandong, China.*

[b]Shandong Provincial Key Lab of Test Technology on Food Quality and Safety, Shandong Academy of Agricultural Sciences, Jinan, 250100, China.

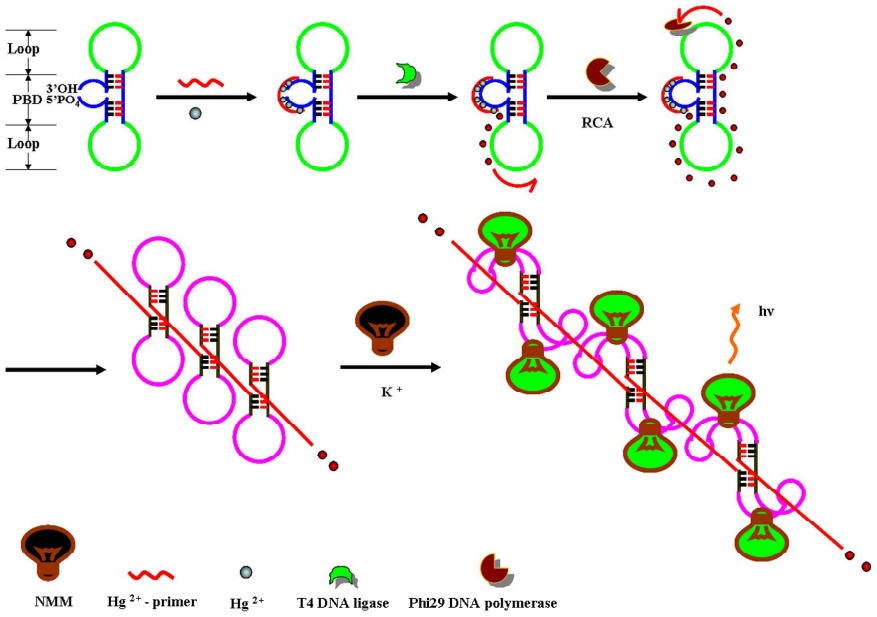

Scheme 1 Schematic representation of the process of the label-free fluorescent sensing system based on target-responsive dumbbell probe-mediated rolling circle amplification (D-RCA) for detection of mercuric ion.

Target-Responsive dumbbell probe-mediated rolling circle amplification strategy for highly sensitive Hg^{2+} detection

Qingwang Xue [a], Yanqin Lv [a], Yuanfu Zhang [a], Shuling Xu [a], Qiaoli Yue [a], Rui Li [a], Lei Wang [a], Haibo Li [a], Xiaohong Gu [b], Shuqiu Zhang[b], Jifeng Liu [a]*

[a] *Department of Chemistry, Liaocheng University, Liaocheng, 252059, Shandong, China.*

[b]*Shandong Provincial Key Lab of Test Technology on Food Quality and Safety, Shandong Academy of Agricultural Sciences, Jinan, 250100, China.*

Corresponding author:

Tel: +86-635-8239001; fax: +86-635-8239001. Email: liujifeng111@gmail.com

Abstract:

A novel label-free amplified fluorescent sensing scheme based on target-responsive dumbbell probe-mediated rolling circle amplification (D-RCA) has been developed for sensitive and selective detection of mercuric ion. In this strategy, we reported an ingeniously designed dumbbell-shaped DNA probe (D-DNA) that integrates target-binding, amplification and signaling within one multifunctional design. An Hg^{2+}-primer DNA (Hg^{2+}-p-DNA) was designed to complementary to the region of D-DNA but with T–T mismatches. The mismatched Hg^{2+}-primer cannot initiate the RCA reaction in the absence of Hg^{2+}. Stable T–Hg^{2+}–T can be formed in the presence of target Hg^{2+}, thus induces the elongation and amplification reaction by a RCA mechanism, resulting in numerous cascade dumbbell probes with duplex G-rich quadruplex structure oligomer. Upon the addition of N-methyl mesoporphyrin IX (NMM), the signal reporter, the strong interaction between the G-quadruplex and NMM brings about a great fluorescence enhancement. In this way, we successfully converted each Hg^{2+}-triggered D-RCA reaction event into the detectable fluorescent signals, which were significantly amplified by RCA in an isothermal fashion. This approach can detect 80 fM mercuric ions, much lower than those of previously reported biosensors, and exhibits high discrimination ability. More significantly, the dynamic range of D-RCA is extremely large, covering 5 orders of magnitude. We also demonstrate Hg^{2+} quantification with this highly sensitive and selective D-RCA strategy in real samples.

Keyword: Hg^{2+} detection; G-quadruplex; label-free; dumbbell probe-mediated rolling circle amplification.

1. Introduction

Mercuric ion (Hg^{2+}), one of the most toxic heavy metal ions and a severe environmental pollutant that is not biodegradable, has serious deleterious effects on human health, especially in the central nervous system, even at low concentration[1, 2]. So far, several modern analytical techniques for mercury detection have been established, such as atomic absorption/emission spectroscopy[3], selective cold vapor atomic fluorescence spectrometry[4, 5] and inductively coupled plasma mass spectrometry (ICP-MS)[6]. However, most of them require expensive and sophisticated instrumentation and/or complicated sample preparation processes. Alternatively, chemical sensors based on small organic fluorophores for Hg^{2+} are easy and rapid to operate.[7-10] But many of these systems are limited in practical use, due to their poor sensitivity[11, 12], strong dependence on organic solvents [13, 14] and cross-sensitivities toward other metal ions[15].

The recent discovery of Hg^{2+}-mediated thymine–thymine (T–T) DNA base-pairing provides an efficient platform for constructing highly selective sensing systems for highly selective Hg^{2+}detection by using T-containing oligonucleotides[15-17]. Numerous Hg^{2+} detection methods including fluorescent[18, 19], colorimetric, and electrochemical biosensor have been developed[20-24]. Among them, the development of homogeneous fluorescence sensors is one of the most attractive and interesting areas due to its simplicity and rapidness [25-28]. Recently, several fluorescent sensing systems based on molecular beacon[29], linear quencher–fluorophore probes,[30, 31] graphene

oxide[32], gold nanorods[33], conjugates polymers and carbon nanomaterial [34, 35] have been reported for Hg^{2+} assay. These methods mainly relied on the fluorescence resonance energy transfer (FRET) process. Although these methods possess high sensitivity and selectivity, these methods require at least one end tag modification of DNA probe. The requirement of fluorescently labeled probes increases the experimental cost and the design complexity, making the assays time-consuming, laborious and cost-intensive.[36, 37] To circumvent the aforementioned limitations, a kind of DNA intercalators (SYBR Green I, TOTO-3 and YOYO-1), specific fluorometric dyes, were used to develop label-free Hg^{2+} sensor[38]. Recently, Xing developed a new label-free Hg^{2+} ions assay with polymerase assisted fluorescence amplification, resulting in a low detection limit of 40 pM and high specificity[39]. However, there is a dispute about the toxicity of some intercalation dyes. In theory, intercalation dyes are not safe enough and may be a threat to the health of the operators[29]. Recently, Feng *et al* developed a novel label-free fluorescent sensor for Hg^{2+} based on target-induced structure-switching of G-quadruplex.[40] Although the label-free fluorescence method does not require any chemical modification for DNA, it shows poor detection limits with 25 nM, which can hardly meet the demanded sensitivity which is below 10 nM (the maximum contamination level defined by the US Environmental Protection Agency (EPA)). Consequently, the development of a novel, label-free and signal-amplified approach for further improving sensitivity and selectivity is highly desirable.

More recently, an isothermal amplification method designated as rolling circle

amplification (RCA), has gained considerable attention as a novel tool to amplify the recognition events detections. Due to the simplicity, robustness and high signal amplification of RCA, numerous novel methods based on RCA has been popularly employed in DNA,[41] RNA,[42] and protein[43] detection. Xing firstly reported a novel electrochemiluminescent sensor for Hg^{2+} detection by using padlock probe-based RCA, resulting in a detection limit of 100 pM.[44] Although the assay exhibits acceptable sensitivity and high specificity, the approaches need the complex labeling procedure and chemical modification for DNA, making the assays time-consuming, laborious and cost-intensive. Consequently, the development of a novel, label-free and signal-amplified approach for further improving sensitivity and selectivity is highly desirable.

In this study, we developed a novel label-free fluorescent amplification sensing scheme based on target-triggered dumbbell probe-mediated rolling circle amplification (D-RCA)-responsive G-quadruplex formation for highly sensitive and selective detection of Hg^{2+}. A dumbbell-shaped DNA probe (D-DNA) that integrates target-binding, amplification and signaling within one multifunctional design was ingeniously designed. Hg^{2+}-primer DNA (Hg^{2+}-p-DNA) was designed to complementary to the region of D-DNA but with T–T mismatches. It can initiate rolling circle amplification (D-RCA) in the presence of Hg^{2+} target, resulting in numerous cascade dumbbell probes with duplex G-rich quadruplex structure oligomer. Upon the addition of N-methyl mesoporphyrin IX (NMM), the strong interaction between the G-quadruplex and NMM brings about a great fluorescence enhancement

for Hg^{2+} detection. The scheme takes advantage of the highly specific T-Hg^{2+}-T complex-dependence of the DNA hybridization, the powerful signal amplification capability of RCA and the significant increase of the fluorescence signal from the interaction between N-methyl mesoporphyrin IX (NMM) and G-quadruplexes. NMM is a commercially available unsymmetrical anionic porphyrin characterized by a pronounced structural selectivity for G-quadruplex forms. It is weakly fluorescent, but exhibits a prominent enhancement in its fluorescence upon binding to G-quadruplex DNA. We aim to improve the sensitivity of Hg^{2+} detection via RCA and the selectivity by using the dumbbell probe to reduce non-specific amplification and the highly specific T-Hg^{2+}-T complex-dependence of the DNA hybridization. In addition, we achieve the label-free by the strong interaction between the G-quadruplex and NMM.

Scheme 1

2. EXPERIMENTAL SECTION

2.1 Materials and Reagents

Phi29 DNA polymerase, T4 DNA ligase, and dNTP were obtained from Fermentas (Lithuania). The oligonucleotides with the following sequences were obtained from Shanghai Sangon Biological Engineering Technology & Services Co., Ltd. (China): the dumbbell probe (D-DNA): 5'-TCTTTCTTCCGA CATCAACCCA AAACCCAAAA CCCAAAAC CCAAG ATGTCGC ACGCTAAA CCC AAA ACCC AA AACCCAAAAC CCAATA GCGT GGTGTTTCCT-3'. Hg^{2+}- specific primer

DNA (Hg^{2+}-p-DNA): 5'-CTTGTTTGTT GGTTTCTC-3'. The Hg^{2+} stock solution (1.0×10^{-3} M) was prepared in ultrapure water with 2 drops of concentrated nitric acid. Other chemicals (analytical grade) were obtained from standard reagent suppliers. Water ($\geqslant$18.2M) was used and sterilized throughout the experiments. N-methyl mesoporphyrin IX (NMM) was purchased from J&K Scientific Ltd. (Beijing, China).

2.2 Apparatus

All the fluorescence measurements were performed on a Hitachi F-7000 spectrofluorimeter (Hitachi, Japan). The excitation wavelength was 399 nm, and the spectra are recorded between 600 and 620 nm. The fluorescence emission intensity was measured at 608 nm.

2.3 Ligation reactions

The ligation reaction was carried out with 20 μl of a reaction mixture [40 mM Tris-HCl, 10 mM $MgCl_2$, 10 mM dithiothreitol (DTT) (pH 7.8), 500 mM ATP, 75 nM the dumbbell probe (D-DNA) and 25 nM Hg^{2+}-p-DNA]. Before adding T4 DNA ligase, the oligonucleotide mixture was firstly denatured at 95 °C for 3min, and cooled slowly to room temperature over a 10-min period. Then, the reaction mixture was incubated to hybridize at 37 °C for 30 min in the presence of 5 μL Hg^{2+} solution of different concentration. Then, 1 μL (5 U) T4 DNA ligase was added to the mixture and incubated at 37 °C for 2 h. The full hybridization equilibrium between the D-DNA and p-DNA is a key factor for ensuring effcient ligation reaction. Therefore, the effect of molar ratio of the D-DNA to p-DNA was evaluated in **Fig. S1**(see

156 supporting information).

157 **2.5 RCA reactions**

158 For RCA, the aforementioned ligation product was mixed with 4 μL 10 ×
159 reaction buffer [330 mM Tris-acetate, 100 mM $Mg(Ac)_2$, 660 mM Potassium Acetate
160 (KAc), 1% Tween 20 and 10 mM DTT (pH 7.9)], 2 μL (10 u/μL) phi29 DNA
161 polymerase and 8 μl 10 mM dNTPs. The reaction mixture was incubated at 37 ℃ for
162 120 min.

163 **2.6 Measurement of fluorescent spectra**

164 The RCA amplification product was mixed with 5 μL 250 μM N-methyl
165 mesoporphyrin IX (NMM) and 5 μL 470 mM KCl, final volume of 50 μl. The
166 reaction mixture was incubated at 37 ℃ for 30 min. The fluorescent spectra were
167 measured using a spectrofluorophotometer. The excitation wavelength was 399 nm,
168 and the spectra are recorded between 600 and 620 nm. The fluorescence emission
169 intensity was measured at 608 nm.

170

171 **3. Results and discussion**

172 **3.1 Sensing strategy**

173 The designed strategy is conceptually depicted in Scheme 1. The dumbbell
174 padlock probe (D-DNA) with two stem-loop structures was chosen as RCA unit for
175 the amplified sensing system based on its high sensitivity and selectivity. The D-DNA
176 three kinds of domains, a Hg^{2+}-specific primer-binding domain (Hg^{2+}-PBD), a stem
177 domain and two loop domains. Hg^{2+}-specific primer (Hg^{2+}-p-DNA) can be hybridized

178 to the dumbbell padlock probe template in the presence of Hg^{2+} based on T-Hg^{2+}-T
179 construction. Phi29 DNA polymerase can initiate the RCA reaction, resulting in
180 numerous cascade dumbbell probes with duplex G-rich oligomer. This G-rich
181 oligomer fold into a quadruplex structure with monovalent ions. Upon the addition of
182 NMM, the signal reporter, the strong interaction between the "activated"
183 G-quadruplex and NMM brings about a great fluorescence enhancement. Eventually,
184 RCA provides an amplified detection signal for the target Hg^{2+}. In contrast, in the
185 absence of target Hg^{2+}, Hg^{2+}-p-DNA can not be hybridized to the template D-DNA,
186 and the RCA process could not proceed. Therefore, there was no fluorescence. In this
187 way, we successfully converted each Hg^{2+}-triggered RCA reaction event into the
188 detectable fluorescent signals, which were significantly amplified by RCA in an
189 isothermal fashion.

190 **3.2 The verification of the sensing strategy**

191 In this novel strategy, RCA was a crucial step, which mediated the generation
192 and amplification of the fluorescence signal. To verify the amplification of the RCA
193 reaction, the agarose gel electrophoresis experiment was performed. The RCA
194 products were investigated by gel electrophoresis. It is observed that the RCA
195 products in lane 2-3 reaction show extremely low mobility in **Fig. 1A**. The anticipated
196 high molecular weight of RCA product was confirmed in lane 2, 3. Compared with
197 lane 2, 3, lane 1 displayed no bands in negative control experiment. These results give
198 immediate evidence for the high molecular weight of these products, indicating Hg^{2+}
199 acted as a trigger of the RCA reaction and the signal enhancement had a positive

correlation with the Hg^{2+} level. In addition, the amplification of the RCA reaction was also verified using fluorescent intensity. Typical fluorescence spectra characteristics of the sensing strategy in response to Hg^{2+} are shown in **Fig. 1B**. Compared with the background fluorescence of the NMM, 10 nM Hg^{2+} resulted in a significant fluorescence enhancement while a control experiment without Hg^{2+} only exhibited a negligible fluorescence change. The result provided a convincing proof of the detection mechanism of the proposed sensing strategy shown in Scheme1.

Fig. 1.

3.3 Optimization of parameters-dependent signal amplification of the sensing strategy

In order to achieve the system's best sensing performance, several experimental parameters affecting RCA were investigated. The full hybridization equilibrium between the Hg^{2+}-p-DNA and D-DNA is a key factor for ensuring RCA reaction. Therefore, the effect of the concentration of Hg^{2+}-p-DNA was evaluated. As shown in **Fig. S2A** (see supporting information), the fluorescence intensity increased with the increase of the concentration of Hg^{2+}-p-DNA. When the concentration of Hg^{2+}-p-DNA reached 10 nM, the maximum fluorescence intensity was achieved. Thereafter, the fluorescence response exhibited a gradual decrease with a further increase of the concentration of Hg^{2+}-p-DNA. This was probably because a large excesses of Hg^{2+}-p-DNA disturbed their hybridization with the D-DNA in a head-to-tail fashion and the subsequent D-RCA reaction.[45] As a result, 10 nM was selected as the optimal concentration of Hg^{2+}-p-DNA due to its strongest fluorescence

intensity. In theory, more complementary copies (duplex G-quadruplexes DNA) of the dumbbell probes template are generated with the elongation of RCA reaction time; stronger signal amplification will be produced. So the effect of RCA reaction time on the fluorescence signal was examined, which is shown in **Fig. S2B** (see supporting information). The fluorescence intensity enhanced quickly with the increase in reaction time, and nearly reached a plateau after 120 min. This might be attributed to the fact that the RCA reaction had reached equilibrium caused by exhaustion of the RCA substrates or inactivation of phi29 DNA polymerase. Therefore, 120 min was chosen as the optimum time for the RCA reaction. This time was in agreement with the reported RCA reaction time of 1-2 h.

To achieve the best sensing performance, the concentration of NMM and K^+ were also optimized. As shown in **Fig. S2C-D**(see supporting information). The experimental results indicated that a concentration of 100 mM of K^+ and 25 μM of NMM could provide maximum S/N ratio for the sensing system.

3.4 The sensibility and detection range of the designed sensing system

In our study, we evaluated the sensitivity of the Hg^{2+} ions fluorescence sensor under optimized conditions. **Fig. 2A** illustrates fluorescence spectra of sensing system after addition of different concentrations of Hg^{2+} ions (0 - 10 nM) under the optimal conditions. Significantly, the fluorescence intensity gradually increased along with Hg^{2+} ions concentration, leading to an impressively large dynamic range that spans five orders of magnitude (0 to 10 nM). **Fig. 2B** shows the logarithmic relationship between the fluorescence response and the different concentrations of Hg^{2+} ions. The

linear concentration ranges were 100 fM up to 10 nM for Hg^{2+} ions over a 6-decade concentration range with a linear correlation coefficient of 0.992. The calculated limit of low detection is 80 fM for Hg^{2+} ions in terms of the 3σ rule. The detection limit of the newly designed Hg^{2+} ions sensing system is 2-3 orders of magnitude lower than that of previously reported fluorescent methods[38, 39, 46]. The ultrahigh sensitivity was attributed to the following factors. First, the introduction of Hg^{2+} ions would trigger the RCA reaction, and eventually RCA product with many tandem repeated duplex G-quadruplexes was generated in large quantities by RCA, substantially amplifying each target-triggered RCA reaction event. Second, free NMM and D-DNA showed relatively low background fluorescence, which dramatically increased the fluorescence signal-to-noise (S/N) ratio.

Fig. 2.

3.5 The selectivity of this sensing system

Fig. 3.

To test the selectivity of this novel method for Hg^{2+} ions detection, control experiments were executed to evaluate whether other environmentally relevant metal ions performed the similar function as the Hg^{2+} ions in the current biosensor. As revealed in **Fig. 3,** one can find that only the Hg^{2+} ions samples show a significant higher fluorescence intensity relative to the competing metal ions samples at identical conditions. The competing metal ions exhibited almost the same fluorescence response as the blank solution without target, and did not induce any significant signal. In addition, the co-existence of other metal ions with Hg^{2+} in the sample also did not

affect Hg^{2+} detection **(Fig.4).** This result obviously indicated that the proposed strategy had suffcient selectivity in Hg^{2+} ions detection. The high selectivity makes it promising for practical applications. The excellent specificity was attributed to using the dumbbell probe to reduce non-specific amplification and the highly specific T-Hg^{2+}-T complex-dependence of the DNA hybridization.

Fig. 4.

3.6 Application of designed sensing system in the real samples

In order to verify the usefulness of the proposed sensor for the identification and detection of Hg^{2+} in practical applications, the detection of natural Hg^{2+} in real samples (tap water, orange juice, and lake water) was demonstrated here by the use of the designed sensing system. The samples collected were first centrifuged for 10 min at 10000 rpm, then filtered through a 0.22 μm membrane and detected according to the general procedure with three replicates. Prior to the assay, the samples were diluted 10 times with ultrapure water so that the level of Hg^{2+} was within the linear ranges. The results averaged from three determinations are summarized in Table 1 (in supporting information). The data listed in **Table 1**(see supporting) indicated that the obtained results were highly consistent with those from the atomic fluorescence spectrometry (AFS) method. Meanwhile, when the known amount of Hg^{2+} was added in these samples, the recovery of Hg^{2+} ranged from 98% to 107%. These confirm that the designed sensor has a high accuracy and sensitivity to meet the requirements of the application.

Table 1

4. Conclusions

In summary, we have successfully demonstrated a novel label-free fluorescent sensing scheme based on target-responsive dumbbell probe-mediated rolling circle amplification (D-RCA) for sensitive and selective detection of Hg^{2+} ions monitoring. The label-free cascade fluorescence amplification strategy shows promising capabilities of specific and sensitive analysis for Hg^{2+} ions detection. The advantages of the strategy include: (i) an extremely low detection limit as low as 80 fM for Hg^{2+} ions is respectively achieved. More significantly, the dynamic range of the based on Hg^{2+}-mediated D-RCA is extremely large, covering 6 orders of magnitude; (ii) this label-free design does not require any chemical modification for DNA or sophisticated equipments, which offers the advantages of simplicity and cost efficiency. (iii) The strong T-Hg^{2+}-T interaction and the uniquely designed dumbbell probe ensure the advantages of excellent specificity and reduce non-specific amplification. In addition, the label-free cascade fluorescence amplification strategy based on D-RCA strategy shows a high accuracy for the application. We expect that this highly sensitive and inexpensive D-RCA strategy will become a promising quantification method in both environmental and food safety fields.

Acknowledgements

This project was supported by the Natural Science Foundation of China for Funding (21305058, 21005036, 21075058, 21127006). This work was also supported by Natural Science Foundation (ZR2010BZ004, JQ201106, 2013SJGZ07). This work

was also supported by Shandong Academy of Agricultural Sciences.

References

1. P. E. Koulouridakis and N. G. Kallithrakas-Kontos, *Anal Chem*, 2004, **76**, 4315-4319.
2. L. Magos and T. W. Clarkson, *Annals of clinical biochemistry*, 2006, **43**, 257-268.
3. J. V. Cizdziel and S. Gerstenberger, *Talanta*, 2004, **64**, 918-921.
4. S. Diez and J. M. Bayona, *Journal of chromatography*, 2002, **963**, 345-351.
5. K. Leopold, L. Harwardt, M. Schuster and G. Schlemmer, *Talanta*, 2008, **76**, 382-388.
6. P. Jitaru and F. C. Adams, *Journal of chromatography*, 2004, **1055**, 197-207.
7. R. Metivier, I. Leray and B. Valeur, *Chemistry*, 2004, **10**, 4480-4490.
8. S. Pandey, A. Azam, S. Pandey and H. M. Chawla, *Organic & biomolecular chemistry*, 2009, **7**, 269-279.
9. H. N. Kim, M. H. Lee, H. J. Kim, J. S. Kim and J. Yoon, *Chemical Society reviews*, 2008, **37**, 1465-1472.
10. M. Kumar, N. Kumar, V. Bhalla, H. Singh, P. R. Sharma and T. Kaur, *Organic letters*, 2011, **13**, 1422-1425.
11. C. Y. Li, X. B. Zhang, L. Qiao, Y. Zhao, C. M. He, S. Y. Huan, L. M. Lu, L. X. Jian, G. L. Shen and R. Q. Yu, *Anal Chem*, 2009, **81**, 9993-10001.
12. M. Tian and H. Ihmels, *Chemical communications (Cambridge, England)*, 2009, 3175-3177.
13. Y. K. Yang, K. J. Yook and J. Tae, *J Am Chem Soc*, 2005, **127**, 16760-16761.
14. J. Du, J. Fan, X. Peng, P. Sun, J. Wang, H. Li and S. Sun, *Organic letters*, 2010, **12**, 476-479.
15. E. M. Nolan and S. J. Lippard, *Chemical reviews*, 2008, **108**, 3443-3480.
16. A. Ono and H. Togashi, *Angewandte Chemie (International ed*, 2004, **43**, 4300-4302.
17. Y. Tanaka, S. Oda, H. Yamaguchi, Y. Kondo, C. Kojima and A. Ono, *J Am Chem Soc*, 2007, **129**, 244-245.
18. M. Kumar and P. Zhang, *Biosensors & bioelectronics*, 2012, **25**, 2431-2435.
19. W. S. Han, H. Y. Lee, S. H. Jung, S. J. Lee and J. H. Jung, *Chemical Society reviews*, 2009, **38**, 1904-1915.
20. K. G. a. T. Sarkar, *Supramolecular Chemistry*, 2012, **24**, 748.
21. A. W. Czarnik, *ACS Symposium Series 538; American Chemical Society: Washington DC,*, 1993.
22. D. B. F. A. P. de Silva, A. J. Huxley and T. S. Moody, Coord., *Chem. Rev*, 2000, **205**, 41.
23. J. M. K. L. N. Neupane, C. R. Lohani and K. H. Lee,, *J. Mater. Chem.*, 2012, **22**, 4003.
24. H. F. Wang and S. P. Wu, *Tetrahedron*, 2013, **69**, 1965.
25. C. W. Liu, C. C. Huang and H. T. Chang, *Anal Chem*, 2009, **81**, 2383-2387.
26. N. Dave, M. Y. Chan, P. J. Huang, B. D. Smith and J. Liu, *J Am Chem Soc*, 2010, **132**, 12668-12673.
27. H. Li, J. Zhai, J. Tian, Y. Luo and X. Sun, *Biosensors & bioelectronics*, 2011, **26**, 4656-4660.
28. L. Zhang, T. Li, B. Li, J. Li and E. Wang, *Chemical communications (Cambridge, England)*, 2010, **46**, 1476-1478.

29. H. Xu, X. Zhu, H. Ye, L. Yu, X. Liu and G. Chen, *Chemical communications (Cambridge, England)*, 2011, **47**, 12158-12160.
30. G. Zhu, Y. Li and C. Y. Zhang, *Chemical communications (Cambridge, England)*, 2013, **50**, 572-574.
31. J. Liu and Y. Lu, *Angewandte Chemie (International ed*, 2007, **46**, 7587-7590.
32. J. R. Zhang, W. T. Huang, W. Y. Xie, T. Wen, H. Q. Luo and N. B. Li, *The Analyst*, 2012, **137**, 3300-3305.
33. G. Chen, Y. Jin, L. Wang, J. Deng and C. Zhang, *Chemical communications (Cambridge, England)*, 2011, **47**, 12500-12502.
34. Q. Wang, W. Wang, J. Lei, N. Xu, F. Gao and H. Ju, *Anal Chem,* **2013**, **85**, **12182-12188**.
35. I. B. Kim and U. H. Bunz, *J Am Chem Soc*, 2006, **128**, 2818-2819.
36. Y. Wu, S. Zhan, L. Xu, W. Shi, T. Xi, X. Zhan and P. Zhou, *Chemical communications (Cambridge, England)*, 2011, **47**, 6027-6029.
37. Q. Xue, L. Wang and W. Jiang, *Chemical communications (Cambridge, England)*, 2013, **49**, 2640-2642.
38. B. Liu, *Biosensors & bioelectronics*, 2008, **24**, 762-766.
39. X. Zhu, X. Zhou and D. Xing, *Biosensors & bioelectronics*, 2011, **26**, 2666-2669.
40. Y. Bai, F. Feng, L. Zhao, Z. Chen, H. Wang, Y. Duan, *Anal. Methods*, 2014, **6**, 662-665
41. A. Cao and C. Y. Zhang, *Anal Chem*, 2012, **84**, 6199-6205.
42. Y. Zhou, Q. Huang, J. Gao, J. Lu, X. Shen and C. Fan, *Nucleic Acids Res*, 2010, **38**, e156.
43. Q. Xue, L. Wang and W. Jiang, *Chemical communications (Cambridge, England)*, 2010, **48**, 3930-3932.
44. X. Zhou, Q. Su and D. Xing, *Analytica chimica acta*, 2012, **713**, 45-49.
45. Y. Zhao, L. Qi, F. Chen, Y. Dong, Y. Kong, Y. Wu and C. Fan, *Chemical communications (Cambridge, England)*, 2012, **48**, 3354-3356.
46. L. Qi, Y. Zhao, H. Yuan, K. Bai, Y. Zhao, F. Chen, Y. Dong and Y. Wu, *The Analyst*, 2012, **137**, 2799-2805.

395
396
397 **Figure captions**

398 **Scheme 1** Schematic representation of the process of the label-free fluorescent
399 sensing system based on target-responsive dumbbell probe-mediated rolling circle
400 amplification (D-RCA) strategy for detection of mercuric ion.

401

402 **Fig. 1.** (A) Agarose gel (0.7%) electrophoresis experiments. The products of RCA
403 reaction (1 h) (indicated by 1-3) were denatured at 95 ℃ for 5 min and quenched with
404 ice-cooled water for 10 min. The marker was indicated by M. Line 1, the control
405 without Hg^{2+}; Line 2-3, the positive with Hg^{2+}. The high molecular weight RCA
406 products are observed in lines 2-3. (B) The fluorescent intensity and fluorescence
407 emission spectra under different conditions: NMM; Hg^{2+}-p-DNA + D-DNA + Hg^{2+}
408 (10 nM) + Phi29 DNA polymerase + dNTPs + NMM; Hg^{2+}-p-DNA + D-DNA +
409 Phi29 DNA polymerase + dNTPs + NMM.

410

411 **Fig. 2.** (A) Fluorescence emission spectra obtained in the dumbbell probe-mediated
412 RCA label-free cascade amplification strategy for detection of Hg^{2+} ions with varying
413 concentrations from 0 - 10 nM. (B) Linear relationship between the fluorescent
414 intensity and the concentration of Hg^{2+} ions. Each data point represents an average of
415 6 measurements (each error bar indicates the standard deviation)

416

417

418 **Fig. 3.** Selectivity of the label-free cascade amplification strategy for Hg^{2+} ions
419 compared to other tested metal ions, respectively.

Fig. 4. Fluorescence intensity obtained in the different solutions. (a) 10 nM Hg^{2+} in the standard solution, (a') 10 nM Hg^{2+} in a mixture solution, (b) the standard solution as control, (b') the mixture solution. The mixture solution containing a mixture of other metal ions (Mix; Ni^{2+}, Fe^{2+}, Fe^{3+}, Cd^{2+}, Co^{2+}, Cu^{2+},Mn^{2+} , Pb^{2+} and Zn^{2+} (each 100 nM)).

Table 1. Real Detection and Recovery Test of Hg^{2+} in Different Real Samples.

Scheme 1

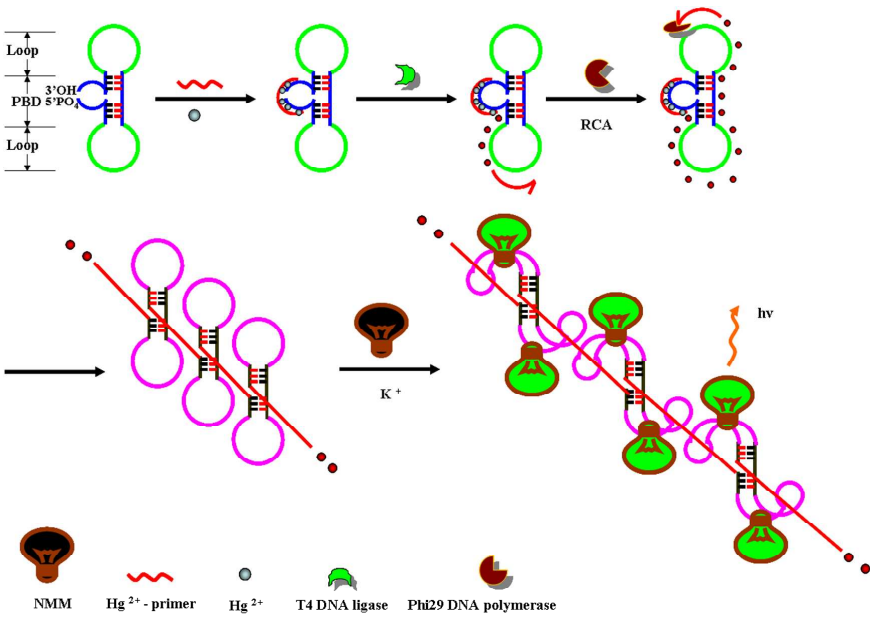

Fig. 1.

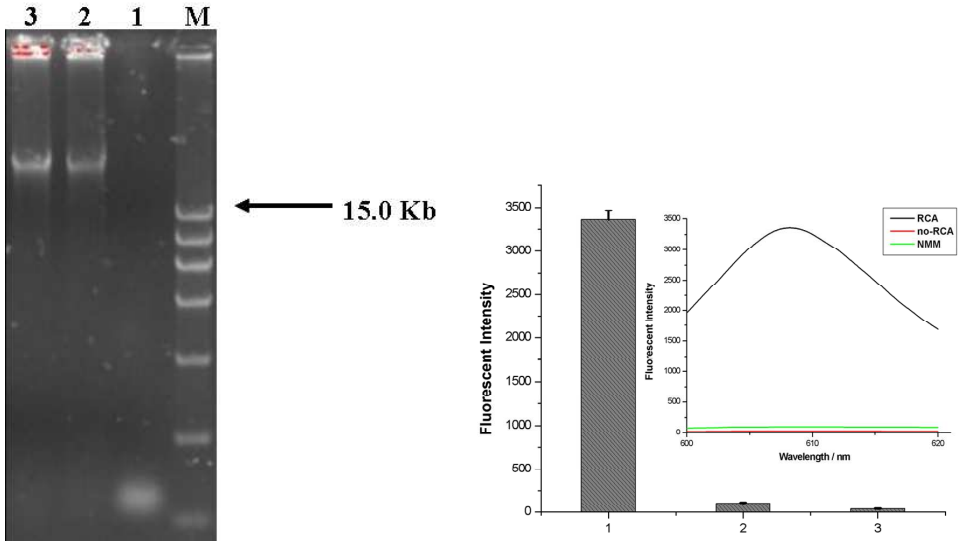

(A) (B)

Fig. 2.

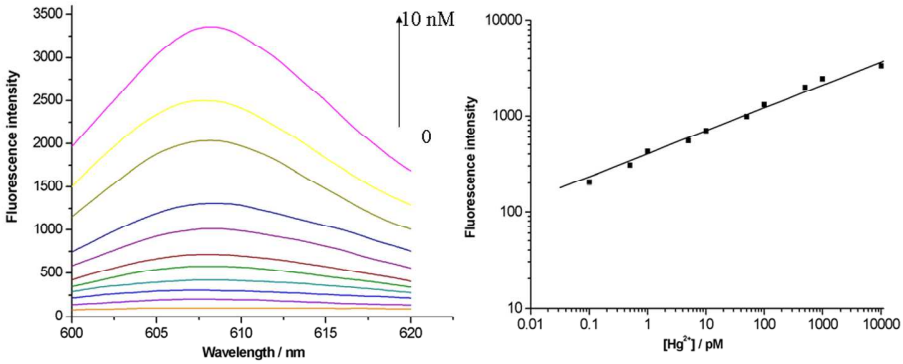

(A) (B)

Fig. 3.

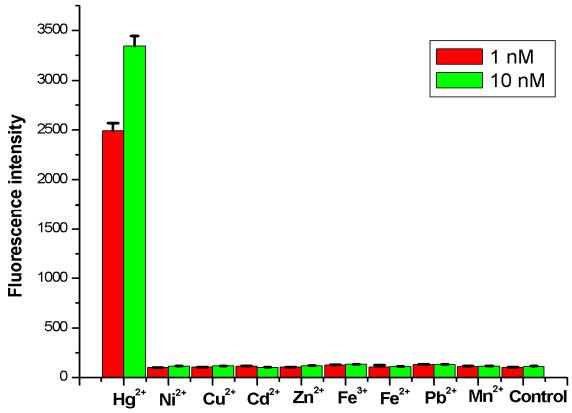

Fig. 4.

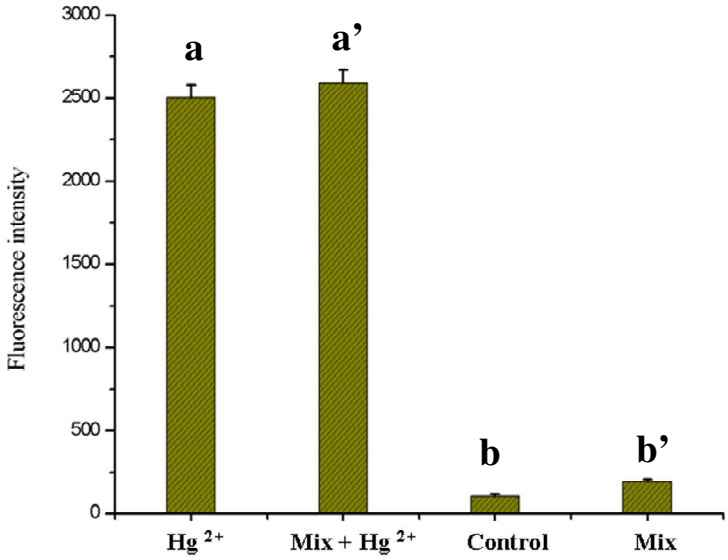

480

481

482 **Table 1.**

Table 1. Real Detection and Recovery Test of Hg^{2+} in Different Samples

sample	AFS method (pM)[a]	proposed method (pM)[b]	spiked Hg^{2+} (pM)	measured Hg^{2-} (pM)	recovery (%)
Orange juice	10.02	1.13	1.0	1.02 ± 0.03	102
Lake water	65.70	6.42	1.0	0.98 ± 0.02	98
tap water	18.5	1.92	1.0	1.07 ± 0.05	107

[a]The data represent natural Hg^{2+} levels detected by standard atomic fluorescence spectrometry.

[b]The Hg^{2+} concentrations were obtained after 10 times dilution with ultrapure water.

483